American Mineralogist, Volume 79, pages 633–643, 1994

In-situ Fe-Mg order-disorder studies and thermodynamic properties of orthopyroxene $(Mg,Fe)_2Si_2O_6$

Hexiong Yang, Subrata Ghose
Mineral Physics Group, Department of Geological Sciences, University of Washington, Seattle, Washington 98195, U.S.A.

Abstract

A systematic in-situ high-temperature study of Fe^{2+}-Mg distribution over the two octahedral sites, M1 and M2, in synthetic orthopyroxenes ($En_{75}Fs_{25}$, $En_{61}Fs_{39}$, $En_{49}Fs_{51}$, $En_{25}Fs_{75}$, and $En_{17}Fs_{83}$) was undertaken at 1000, 1100, 1200, and 1300 K by the single-crystal X-ray diffraction method. The reversal measurements of cation ordering states were made on samples $En_{75}Fs_{25}$, $En_{61}Fs_{39}$, $En_{49}Fs_{51}$, and $En_{17}Fs_{83}$. Because of the orthopyroxene-clinopyroxene phase transition observed at ~1255 K for $En_{17}Fs_{83}$, no site-occupancy determinations at 1300 K were made for $En_{25}Fs_{75}$ and $En_{17}Fs_{83}$. The site occupancies in the Mg-rich sample ($Fs_{25}En_{75}$) at 1300 K are anomalous because of the existence of a transitional structural state prior to a phase transition from the orthopyroxene to the protopyroxene phase. The asymmetry in the distribution of Fe and Mg over M1 and M2 sites is confirmed in the range 1000–1200 K, although it is much less pronounced than that determined from quenched natural samples at lower temperatures (873–1073 K). An analysis of the site-occupancy data based on the regular solution model of Saxena and Ghose (1971) yielded: $\Delta G_{exch} = 7751 + 3.000T$ (±246) J/mol, $W^{M1} = 10230 - 2.065T$ (±164) J/mol, and $W^{M2} = 14775 - 7.575T$ (±624) J/mol, where T is in kelvins. All three parameters are temperature-dependent, with ΔG_{exch} increasing and W^{M1} and W^{M2} decreasing with increasing temperature. The $W^{M1} - W^{M2}$ term increases with increasing temperature, in accord with the result of Shi et al. (1992) but in contrast to most previous studies. This result suggests that the atomic configurations around the cations in M1 and M2 sites become more dissimilar, and the asymmetry of the orthopyroxene solid solution increases at elevated temperatures (1000–1200 K). The sublattice (Shi et al., 1992) and the regular solution models (Saxena and Ghose, 1971), respectively, were used to derive the microscopic and macroscopic excess thermodynamic parameters (ΔG^{ex}, ΔH^{ex}, and ΔS^{ex}) and the activity-composition relations. The macroscopic excess parameters show positive deviations from ideal mixing. The ΔG^{ex} and ΔH^{ex} values agree reasonably well with those determined experimentally.

Introduction

The $(Mg,Fe)_2Si_2O_6$ orthopyroxenes are major constituents of the Earth's crust and the upper mantle. The two end-members, ferrosilite, $Fe_2Si_2O_6$, and enstatite, $Mg_2Si_2O_6$, form a complete solid solution, which is stable over a wide range of temperature and pressure. The crystal structure of orthopyroxene consists of two nonequivalent SiO_4 tetrahedral sites, A and B, and two crystallographically distinct MO_6 octahedral sites, M1 and M2 (M = Fe, Mg, etc.). The Fe-Mg order-disorder between M1 and M2 sites is of special interest because it is closely related to the cooling history of host rocks and to the excess thermodynamic properties of the orthopyroxene solid solution.

The intracrystalline Fe-Mg distribution in natural orthopyroxenes quenched at various temperatures has been extensively investigated by means of ^{57}Fe Mössbauer resonance spectroscopy and single-crystal X-ray diffraction techniques (e.g., Evans et al., 1967; Ghose and Hafner, 1967; Virgo and Hafner, 1969; Saxena and Ghose, 1971; Domeneghetti et al., 1985; Sykes and Molin, 1986; Molin et al., 1991; Hazen et al., 1993). Some kinetic experiments were undertaken to explore the possibility of using the Fe-Mg ordering states in orthopyroxenes as indicators of cooling rates (Besancon, 1981; Anovitz et al., 1988; Saxena et al., 1989; Skogby, 1992; Sykes-Nord and Molin, 1993). Paralleling the development of that experimental research, the thermodynamic behavior of the orthopyroxene solid solution as a function of chemical composition, temperature, and pressure has been modeled by several workers (e.g., Saxena and Ghose, 1971; Navrotsky, 1971; Sack, 1980; Davidson and Lindsley, 1985, 1989; Sack and Ghiorso, 1989; Akamatsu, 1989; Shi et al., 1992). However, all previous cation ordering data were obtained from quenched natural samples, which poses several complications in the correct derivation of the thermodynamic properties of orthopyroxenes. First,

0003–004X/94/0708–0633$02.00

natural crystals always contain small amounts of other cations in addition to Mg^{2+}, Fe^{2+}, and Si^{4+}, such as Ca^{2+}, Mn^{2+}, Al^{3+}, Cr^{3+}, Ti^{4+}, etc. As indicated by Snellenburg (1975), Hawthorne and Ito (1977), Domeneghetti et al. (1985), Molin (1989), and Sykes-Nord and Molin (1993), the presence of these minor elements can cause significant changes in some structural parameters and physical properties. Among all the minor elements, Al is the most critical because it can substitute for both Si in the tetrahedral sites and (Mg,Fe) in the octahedral sites. Second, natural orthopyroxenes often contain submicroscopic exsolution lamellae of Ca-rich pyroxenes and other oxide phases, which can be partially resorbed in the host phase during heating at a given temperature. Third, it has been demonstrated that the kinetics of intracrystalline Fe-Mg fractionation is very rapid at high temperature and that the cation equilibrium ordering states above 900 °C are unquenchable (Besancon, 1981; Anovitz et al., 1988). Consequently, the previously determined Fe-Mg equilibrium distribution data in quenched samples are diverse (Anovitz et al., 1988), and the thermodynamic parameters derived from experimental data are quite different (see e.g., Sack and Ghiorso, 1989; Shi et al., 1992).

In this paper, we present the first systematic in-situ high-temperature studies of Fe-Mg order-disorder in synthetic $(Fe,Mg)_2Si_2O_6$ orthopyroxenes at 1000, 1100, 1200, and 1300 K by the single-crystal X-ray diffraction method. Our results suggest that the Fe-Mg equilibrium distribution data above 1250 K are anomalous and not suitable for thermodynamic modeling because of the orthopyroxene to clinopyroxene phase transition observed at ~1255 K in Fe-rich orthopyroxenes. The Fe-Mg order-disorder at 1300 K in Mg-rich orthopyroxenes is also anomalous because of a transitional structural state (Yang and Ghose, in preparation). The asymmetric distribution of Fe and Mg over the M1 and M2 sites in the range 1000–1200 K is confirmed, although it is much less pronounced than that found in the previous work from natural samples quenched at lower temperatures (873–1073 K). Thermodynamic parameters of the orthopyroxene solid solution, including activity-composition relations, are derived from the present Fe-Mg distribution data.

Previous work

The strong partitioning of Fe and Mg over the two nonequivalent octahedral sites, M1 and M2, in a natural orthopyroxene was first observed from single-crystal X-ray diffraction studies by Ghose (1965), who also predicted the temperature dependence of the cation partitioning. Evans et al. (1967), Ghose and Hafner (1967), and Saxena and Ghose (1970) reported Fe-Mg distribution in plutonic and volcanic orthopyroxenes by ^{57}Fe Mössbauer resonance. Ghose and Hafner (1967) also reported site occupancies in some orthopyroxenes quenched from 1000 and 1100 °C. Following Mueller (1962), Ghose and Hafner (1967) presented the intracrystalline cation distribution by an ion-exchange equation for Mg and Fe between M1 and M2 sites:

$$RT \ln K_D = -\Delta G_{exch} \quad (1)$$

and

$$K_D = \frac{X_{Fe}^{M1} X_{Mg}^{M2}}{X_{Fe}^{M2} X_{Mg}^{M1}} \quad (2a)$$

where K_D is the intersite cation distribution constant for the following exchange reaction:

$$Mg(M1)Fe(M2)Si_2O_6 \rightleftharpoons Fe(M1)Mg(M2)Si_2O_6. \quad (2b)$$

Virgo and Hafner (1969) determined the Fe-Mg distribution isotherm at 1000 °C in quenched samples and the kinetics of the Fe-Mg order-disorder of an intermediate orthopyroxene (X_{Fe} = 0.57) at 500, 600, 700, 800, and 1000 °C by Mössbauer resonance spectroscopy. They assumed an ideal distribution of Fe and Mg between M1 and M2 sites and found that ΔG_{exch} is approximately constant between 600 and 1000 °C. On the basis of the data of Virgo and Hafner (1969), Navrotsky (1971) derived a simple, but not a regular, solution model for the Gibbs free energy of mixing in the orthopyroxene series. In this model, the excess Gibbs free energy (ΔG^{ex}) and the extent of cation ordering are symmetric about X_{Fe} = 0.5. Moreover, nearly ideal thermodynamic behavior of the solution at approximately 1000 °C is expected from this model.

A more systematic study of the Fe-Mg fractionation in orthopyroxenes by ^{57}Fe Mössbauer resonance was performed by Saxena and Ghose (1971). They examined nine natural orthopyroxene samples quenched from 500 to 800 °C and presented a regular solution model. Interaction energy factors W^{M1} and W^{M2} were introduced in this model corresponding to the octahedral sites, M1 and M2, to describe the nonideality of the orthopyroxene solid solution:

$$RT \ln K_D = RT \ln K - W^{M1}(1 - 2X_{Fe}^{M1}) + W^{M2}(1 - 2X_{Fe}^{M2}) \quad (3)$$

where

$$K = \frac{a_{Fe}^{M1} a_{Mg}^{M2}}{a_{Fe}^{M2} a_{Mg}^{M1}} = \exp(-\Delta G_{exch}/RT) \quad (4)$$

and a_{Fe}^{M1} and a_{Fe}^{M2} are the partial activities of Fe on the M1 and M2 sites, respectively, and a_{Mg}^{M1} and a_{Mg}^{M2} are the partial activities of Mg on the M1 and M2 sites, respectively. W^{M1} and W^{M2} were found to be nonequivalent and temperature dependent. Accordingly, this model is known as the asymmetric regular solution model.

Sack (1980) suggested that an additional, Bragg-Williams kind of energy term (ΔG_{rec}) may make a substantial contribution to the deviation from ideal mixing of the solution. In other words, a reciprocal ordering reaction,

$$Fe_2Si_2O_6 + Mg_2Si_2O_6 \rightleftharpoons Fe(M2)Mg(M1)Si_2O_6 + Fe(M1)Mg(M2)Si_2O_6$$

TABLE 1. Sample description and chemical compositions

Sample no.	1	2	3	4	5
Brief notation	Fs25 F*	Fs39	Fs51 F*	Fs75 D*	Fs83 C*
			Oxide (wt%)		
SiO_2	55.623	53.133	51.716	48.392	47.383
MgO	27.994	21.744	17.047	8.153	5.404
FeO	16.546	25.211	31.144	43.342	47.322
Total	100.16	100.09	99.91	99.89	100.11
			Cation numbers (based on six O atoms)		
Si	2.001	1.995	2.003	2.000	1.996
Mg	1.501	1.217	0.985	0.502	0.339
Fe	0.498	0.788	1.012	1.498	1.662
Fe/(Fe + Mg)	0.249	0.394	0.506	0.749	0.831
Sample source**	LY	O	LY	L	LY

* Original notations used by D.H. Lindsley at SUNY, Stony Brook, for different experiments of the same composition.
** LY = Lindsley and Yang, O = Ohashi, L = Lindsley.

should be taken into account to incorporate both the intrasite and intersite interactions into the thermodynamic expression of the orthopyroxene solid solution:

$$RT \ln K_D = RT \ln K + \Delta G_{rec}(X_{Fe}^{M2} - X_{Fe}^{M1}) - \overline{W}^{M1}(1 - 2X_{Fe}^{M1}) + \overline{W}^{M2}(1 - 2X_{Fe}^{M2}). \quad (5)$$

Note that the $\overline{W}^{M1}$ and $\overline{W}^{M2}$ terms in Equation 5 have different physical meanings and numerical values from those in Equation 3. As pointed out by Sack (1980) and Ganguly (1982), the W terms in Equation 3 implicitly contain the ΔG_{rec} term, i.e.,

$$W^{M1} = \overline{W}^{M1} - \tfrac{1}{2}\Delta G_{rec} \quad (6a)$$

$$W^{M2} = \overline{W}^{M2} - \tfrac{1}{2}\Delta G_{rec}. \quad (6b)$$

Equation 5 was used later by Davidson and Lindsley (1985, 1989), Sack and Ghiorso (1989), and Shi et al. (1992).

Despite the numerous studies on orthopyroxenes cited above, some questions regarding the thermodynamic nature of mixing remain. One important question is whether the orthopyroxene solid solution is symmetric or asymmetric. Virgo and Hafner (1969), Navrotsky (1971), Davidson and Lindsley (1985, 1989), and Sack and Ghiorso (1989) treated the solid solution as symmetric, whereas other workers considered the solution to be asymmetric (Saxena and Ghose, 1971; Shi et al., 1992). Another question is how the interaction parameters (W terms) behave with temperature. Shi et al. (1992) employed the theory of sublattice solid solution and optimization methods and found that $W^{M1} - W^{M2}$ increases with increasing temperature, contrary to previous results (e.g., Saxena and Ghose, 1971; Sack, 1980; Davidson and Lindsley, 1985, 1989).

EXPERIMENTAL METHODS

Samples

To avoid complications due to the presence of minor elements in natural orthopyroxenes (Ca, Al, Mn, Cr, Ti, etc.) and their influence on the crystal structure and the Fe-Mg fractionation, we have exclusively used pure synthetic single crystals of orthopyroxenes with the chemical compositions $(Fe_{0.25},Mg_{0.75})_2Si_2O_6$, $(Fe_{0.39},Mg_{0.61})_2Si_2O_6$, $(Fe_{0.51},Mg_{0.49})_2Si_2O_6$, $(Fe_{0.75},Mg_{0.25})_2Si_2O_3$, and $(Fe_{0.83},Mg_{0.17})_2Si_2O_6$. The following abbreviations are used for the samples in this paper: En = enstatite ($MgSiO_3$) and Fs = ferrosilite ($FeSiO_3$) in orthopyroxene solid solutions. For simplicity, we only use the Fs content (%) in orthopyroxenes as the sample designation; for example, $En_{75}Fs_{25}$ is referred to as Fs25. All samples were synthesized hydrothermally in the piston-cylinder apparatus. Samples Fs25, Fs51, Fs75, and Fs83 were synthesized following the crystal growth procedure described by Turnock et al. (1973). Except sample Fs75, which was kindly donated by D. H. Lindsley, and sample Fs39, which was provided by H. Ohashi of Tsukuba, Japan, all samples were grown by D. H. Lindsley and H. Yang at SUNY, Stony Brook. All crystals used for the X-ray diffraction study were chemically analyzed in the JEOL 733 electron microprobe at the University of Washington with a 15-keV accelerating voltage and a 25-nA beam current measured on the Faraday cup. Chemical compositions and other relevant data on the samples are listed in Table 1. The compositional variability of each crystal was also examined by the electron microprobe. All crystals were found to be quite homogeneous, with 1σ for Mg $\approx \pm 0.01$ per six O atoms.

Single crystal X-ray diffraction measurements

A nearly spherical crystal was selected from each sample for both unit-cell dimension and X-ray diffraction intensity measurements. All X-ray diffraction experiments were performed on a large (Huber 512) automated four-circle diffractometer equipped with a graphite-monochromator and using Mo$K\alpha$ radiation (50 kV, 32 mA). A gas-flow furnace designed by Tsukimura et al. (1989) was modified to reach 1350 K with a temperature stability of ± 5 K. The furnace was mounted on an

TABLE 2. Crystal data and site occupancies of orthopyroxenes at various temperatures

	Heating				Cooling			
T (K)	1000	1100	1200	1300	1000	1100	1200	1300
Heating time (h)	36	24	4	2	36	24	4	2
				Fs25				
a (Å)	18.388(2)	18.411(2)	18.432(2)	18.453(3)	18.388(3)	18.409(3)	18.430(3)	18.453(3)
b (Å)	8.958(1)	8.969(1)	8.982(1)	8.991(1)	8.959(1)	8.969(1)	8.983(1)	8.990(2)
c (Å)	5.244(1)	5.254(1)	5.265(1)	5.274(1)	5.243(1)	5.253(1)	5.264(1)	5.275(1)
Total refl.	1859	1865	1878	1883	1853	1863	1874	1888
Refl. > $3\sigma(I)$	702	656	605	518	707	609	570	522
R_w	0.036	0.036	0.042	0.042	0.042	0.037	0.039	0.043
R	0.034	0.035	0.037	0.038	0.039	0.035	0.037	0.035
Fe (M1)*	0.084(3)	0.099(4)	0.115(4)	0.119(5)	0.084(4)	0.097(4)	0.115(4)	0.121(4)
Fe (M2)	0.414	0.399	0.383	0.379	0.414	0.401	0.383	0.377
				Fs39				
a (Å)	18.413(2)	18.432(2)	18.455(3)	18.477(3)	18.412(3)		18.456(3)	
b (Å)	8.977(1)	8.987(1)	8.998(2)	9.008(1)	8.978(1)		8.998(1)	
c (Å)	5.256(1)	5.266(1)	5.276(1)	5.288(1)	5.256(1)		5.275(1)	
Total refl.	1879	1893	1909	1926	1876		1905	
Refl. > $3\sigma(I)$	646	628	560	554	694		539	
R_w	0.041	0.050	0.048	0.045	0.039		0.047	
R	0.033	0.041	0.038	0.036	0.032		0.038	
Fe (M1)	0.181(4)	0.197(4)	0.215(5)	0.230(5)	0.184(3)		0.217(5)	
Fe (M2)	0.607	0.591	0.573	0.558	0.604		0.571	
				Fs51				
a (Å)	18.434(2)	18.453(3)	18.474(3)	18.495(4)	18.432(3)			
b (Å)	9.010(1)	9.020(1)	9.028(1)	9.037(2)	9.011(1)			
c (Å)	5.265(1)	5.276(1)	5.288(1)	5.300(1)	5.265(1)			
Total refl.	1900	1914	1936	1949	1904			
Refl. > $3\sigma(I)$	468	599	550	494	478			
R_w	0.060	0.046	0.046	0.044	0.049			
R	0.049	0.034	0.040	0.033	0.040			
Fe (M1)	0.279(7)	0.296(6)	0.313(6)	0.328(6)	0.282(7)			
Fe (M2)	0.733	0.716	0.699	0.684	0.730			
				Fs75				
a (Å)	18.492(1)	18.518(2)	18.545(3)					
b (Å)	9.083(1)	9.093(1)	9.100(1)					
c (Å)	5.281(1)	5.291(1)	5.304(1)					
Total refl.	2133	2158	2174					
Refl. > $3\sigma(I)$	425	409	320					
R_w	0.030	0.031	0.028					
R	0.033	0.032	0.026					
Fe (M1)	0.587(6)	0.601(6)	0.615(8)					
Fe (M2)	0.911	0.897	0.883					
				Fs83				
a (Å)	18.516(2)	18.540(2)	18.566(2)		18.515(2)	18.541(3)		
b (Å)	9.099(1)	9.108(1)	9.116(1)		9.098(1)	9.107(1)		
c (Å)	5.286(1)	5.297(1)	5.310(1)		5.286(1)	5.298(1)		
Total refl.	2147	2163	2186		2140	2159		
Refl. > $3\sigma(I)$	736	602	526		714	592		
R_w	0.052	0.048	0.046		0.039	0.041		
R	0.047	0.038	0.038		0.038	0.033		
Fe (M1)	0.725(6)	0.736(6)	0.746(6)		0.725(5)	0.735(5)		
Fe (M2)	0.937	0.926	0.916		0.937	0.927		

* Mg (M1) = 1 − Fe (M1); Mg (M2) = 1 − Fe (M2).

x-y-z stage directly across from the goniometer cradle, which is offset by 63.5 mm from the χ-circle plane. Each crystal, along with a small piece of molybdenum wire to absorb residual O, was placed in a silica capillary. The capillaries were then evacuated to $\sim 10^{-2}$ torr and sealed. A Pt and Pt-Rh thermocouple was mounted on the sealed capillary as described by Hazen and Finger (1982). MgO cement was used to glue the parts together. The gas-flow rate was controlled at 2.0 L/min through a flow valve. The temperature calibration was based on the known thermal expansion of NaCl crystal (Enck and Dommel, 1965) and the melting point of Ag.

Before data collection, each crystal was heated at a desired temperature for a certain period that was estimated to be sufficient for the Fe-Mg order-disorder to reach an equilibrium state according to the kinetic studies of the Fe-Mg order-disorder (Besancon, 1981; Anovitz et al., 1988). The heating durations on crystals at various temperatures are listed in Table 2. Subsequently, unit-cell dimensions were determined both upon heating (disordering) and upon cooling (ordering) by least-squares refinements based on 24 reflections with 2θ values between 20 and 35° (Table 2). The X-ray intensity data were collected up to 65° 2θ, with a scan speed of 4.5°/min. For

samples Fs25, Fs39, and Fs51, the data collections were carried out at 1000, 1100, 1200, and 1300 K, whereas for Fs75 and Fs83, the data collections were made at 1000, 1100, and 1200 K because a phase transition from orthopyroxene to clinopyroxene was detected for Fs83 at ~1255 K. To ascertain better the equilibrium Fe-Mg ordering states at a given temperature, reversal X-ray diffraction intensity data collections were conducted at 1000, 1100, 1200, and 1300 K for Fs25, at 1000 and 1200 K for Fs39, at 1000 K for Fs51, and at 1000 and 1100 K for Fs83. The rest of the X-ray intensity data were collected only upon heating.

During all X-ray data collection, the thermal stability of the crystal was monitored by three standard reflections, which were measured after every 97 reflections or at intervals of ~90 min. No significant variations were observed in the intensities of the standard reflections for all X-ray diffraction sets from five samples. After data collection on each crystal, the silica capillary, the crystal, and the molybdenum wire were examined under an optical microscope. No reaction between the crystal and the capillary nor any color change indicating oxidation of the crystal or the molybdenum wire was observed. All X-ray intensity data were corrected for Lorentz and polarization factors. Absorption corrections were made for all crystals by assuming a spherical shape. Only reflections having intensities $\geq 3\sigma(I)$ were considered as observed, where $\sigma(I)$ is the standard deviation determined from the counting statistics. Profiles of all observed reflections were examined. Due to the interference from the thermocouple attached to the silica capillary near the crystal and the powder diffraction rings from the silica rod and the capillary, there are about 30–60 reflections in each data set showing irregular peak shapes or considerably uneven backgrounds. Such reflections were excluded from the subsequent refinements.

Structure refinements and site-occupancy determinations

The initial atomic positional and thermal vibrational parameters of orthopyroxene with the space group *Pbca* were taken from Smyth (1974). The crystal structure refinements were performed using the full-matrix least-squares program RFINE90, which is an updated version of RFINE4 (Finger and Prince, 1975). Neutral atomic scattering factors including anomalous dispersion corrections for Fe, Mg, Si, and O were taken from Ibers and Hamilton (1974). Weighting schemes were based on $w = [\sigma^2(F) + (pF)^2]^{-1}$, where p is the so-called ignorance factor, which is adjustable to achieve a slope of 1 on a probability plot. Site occupancies of Fe and Mg between M1 and M2 were allowed to vary with the bulk chemical composition constrained to that determined from microprobe analysis. In the final cycles of the refinements, the following parameters were refined simultaneously: a scale factor, an isotropic extinction factor (Zachariasen, 1968), atomic positional parameters, anisotropic thermal parameters, and site occupancies of Fe and Mg. The crystal structure at each successive temperature was refined using the parameters from the previous refinement in a similar manner. Final weighted and unweighted discrepancy indices (R_w and R factors) and site occupancies are presented in Table 2.

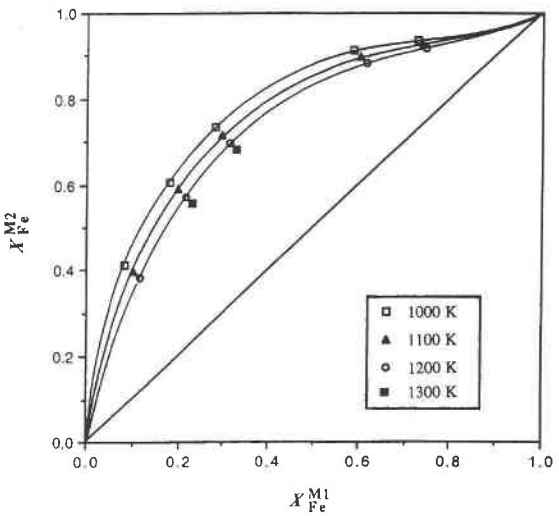

Fig. 1. A Rooseboom plot of site occupancies of Fe between M1 and M2 sites in orthopyroxenes.

Results

The site occupancies as a function of temperature and chemical composition, determined from the final cycles of the structural refinements, are illustrated in the plot of the distribution isotherms of Fe and Mg between M1 and M2 at 1000, 1100, 1200, and 1300 K (Fig. 1).

Mathematically, a regression analysis of the site-occupancy data based on Equation 5 cannot yield unique values for all four parameters, ΔG_{exch}, ΔG_{rec}, $\overline{W}^{M1}$, and $\overline{W}^{M2}$, simultaneously because of the existence of Equation 6. One can vary ΔG_{rec} in a wide range and still get thermodynamically reasonable values for $\overline{W}^{M1}$ and $\overline{W}^{M2}$. In other words, ΔG_{rec}, W^{M1}, and W^{M2} cannot be determined unambiguously from the site-occupancy data alone. Hence, we set $\Delta G_{rec} = 0$ for the following analysis and used Equation 3 to derive ΔG_{exch}, W^{M1}, and W^{M2}. Linear fitting of ΔG_{exch}, W^{M1}, and W^{M2} as a function of temperature yields the following equations:

$$\Delta G_{exch} = 7751 + 3.000T\ (\pm 246)\ \text{(J/mol)} \quad (7)$$

$$W^{M1} = 10230 - 2.065T\ (\pm 164)\ \text{(J/mol)} \quad (8a)$$

$$W^{M2} = 14775 - 7.575T\ (\pm 624)\ \text{(J/mol)} \quad (8b)$$

where the temperature, T, is in kelvins. Figures 2 and 3 are the plots of ln K_D vs. the reciprocal temperature ($1/T$) and the Fe content (X_{Fe}), respectively. Two significant features can be seen from Figures 2 and 3: (1) The ln K_D of Mg-rich orthopyroxene (Fs25) varies nonlinearly with temperature between 1200 and 1300 K (Fig. 2a), in contrast to all previous results. (2) There is a maximum in the curve of the ln K_D vs. X_{Fe} at 1000 K, which corresponds to $X_{Fe} = 0.40$; as the temperature increases, the

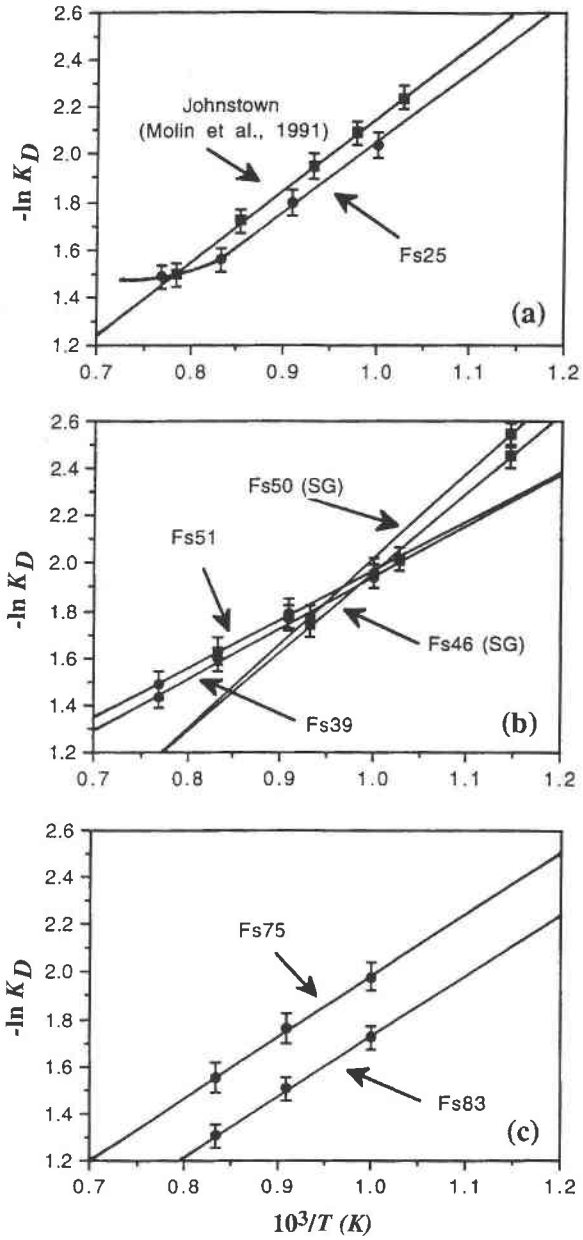

Fig. 2. The ln K_D vs. $1/T$ (K) for orthopyroxenes, with different compositions represented by $\pm 1\sigma$ brackets: (**a**) $(Mg_{0.75}Fe_{0.25})_2Si_2O_6$, (**b**) $(Mg_{0.61}Fe_{0.39})_2Si_2O_6$ and $(Mg_{0.49}Fe_{0.51})_2Si_2O_6$, and (**c**) $(Mg_{0.25}Fe_{0.75})_2Si_2O_6$ and $(Mg_{0.13}Fe_{0.87})_2Si_2O_6$. The data of Molin et al. (1991) from an orthopyroxene with $X_{Fe} = 0.23$ are shown in **a**; the data of Saxena and Ghose (1971) from sample no. 277 (with $X_{Fe} = 0.46$) and sample no. 10 (with $X_{Fe} = 0.50$) are displayed in **b**.

convexity gradually decreases and disappears at 1200 K, but it reappears at 1300 K (Fig. 3) such that the curve of ln K_D vs. X_{Fe} at 1300 K resembles that at 1000 K. Furthermore, for a given composition, the ln K_D value for Fs25 increases at a faster rate (~0.24/100 K) at elevated temperatures than that for the other samples (~0.20/100 K).

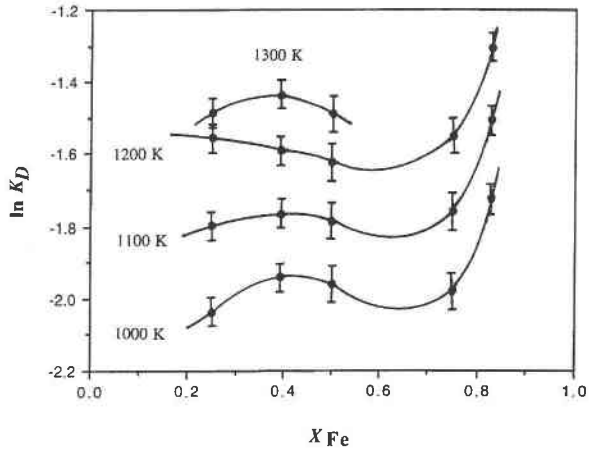

Fig. 3. The ln K_D vs. composition (X_{Fe}) for orthopyroxenes at various temperatures, represented by $\pm 1\sigma$ brackets.

Discussion

Temperature and compositional dependence of the site occupancies and the asymmetry of the Fe^{2+}-Mg distribution isotherms

On the basis of the results obtained from quenched natural samples, Saxena and Ghose (1971) found that the site occupancies of an Fe-rich orthopyroxene with $X_{Fe} = 0.86$ are essentially independent of temperature, resulting in the crossover of the Fe-Mg distribution isotherms between 773 and 973 K. Such a crossover phenomenon was not observed in Fs83 between 1000 and 1200 K in our in-situ measurements. Nevertheless, the asymmetry of the Fe-Mg distribution isotherms, characterized by the change in the curvature in the Rooseboom plot of the Fe distribution between M1 and M2 is confirmed; the curvature is negative for the samples with $X_{Fe} < 0.75$ but becomes positive for the very Fe-rich samples compared with a symmetric distribution curve. This deviation is more pronounced at lower temperatures (773–973 K) in the Fe-Mg distribution isotherms determined by Saxena and Ghose (1971) and indicates a tendency toward antiordering, i.e., a preference of Fe^{2+} for the M1 site rather than for the M2 site in Fe-rich orthopyroxenes that is stronger than an ideal Fe-Mg distribution at the M1 and M2 sites would dictate. The antiordering and, hence, the asymmetric behavior may originate from a small number of $FeSiO_3$ ferrosilite clusters in Fe-rich orthopyroxenes. The cluster size is estimated to be in the 50–100 Å range, which is too small to give distinct X-ray diffraction patterns.

An orthopyroxene to high clinopyroxene ($C2/c$) phase transition detected in Fs83 at ~1255 K (Yang and Ghose, 1994) suggests that it is not possible to extrapolate the site occupancies of Fe-rich orthopyroxenes above 1250 K at 1 bar because the energetics of the cation ordering in high clinopyroxenes (Smyth, 1974) differs from that in orthopyroxenes. Furthermore, a transitional structural state between orthopyroxene and protopyroxene was ob-

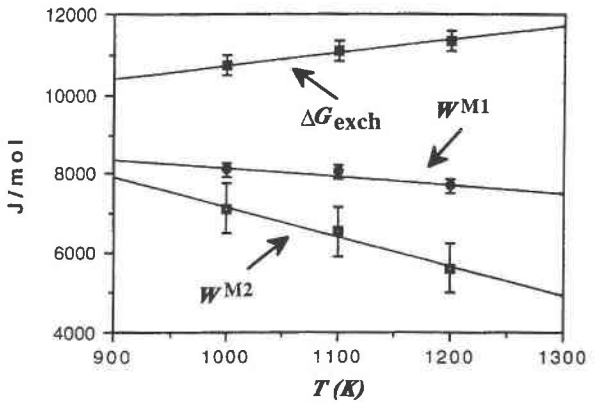

Fig. 4. The exchange Gibbs free energy (ΔG_{exch}) and interaction parameters (W^{M1} and W^{M2}) for M1 and M2 sites in orthopyroxenes as a function of temperature, represented by $\pm 1\sigma$ brackets.

served in Fs25 at 1300 K (Yang and Ghose, in preparation), in which two silicate chain configurations become similar, but the unit-cell dimensions and the space group (*Pbca*) are still those of orthopyroxene. This transitional state is believed to be responsible for the anomalous behavior of the Fe-Mg order-disorder in Fs25 above 1200 K. Thus, it is also inappropriate to extrapolate the site occupancies of Mg-rich orthopyroxenes above ~1250 K at 1 bar.

The anomalous variations of ln K_D with composition and temperature imply that the crystal structures of orthopyroxenes with various compositions respond to temperature differently. The systematic structural analyses of (Fe,Mg) orthopyroxenes show that a more drastic structural change occurs in Mg-rich orthopyroxenes as temperature increases (Yang, 1994). The thermal expansion study of orthopyroxenes (Yang and Ghose, 1994) also reveals that Mg-rich orthopyroxenes show a thermal expansion behavior different from those of the intermediate and Fe-rich orthopyroxenes. Likewise, the energetics of the Fe-Mg ordering in Mg-rich orthopyroxenes appears to be different from that in the Fe-rich orthopyroxenes. The kinetic study of Sykes-Nord and Molin (1993) also suggests that Mg-rich orthopyroxenes respond to temperature differently from Fe-rich ones. Their results show that there is a gap in the activation energies for the Fe-Mg ordering between Mg-rich and Fe-rich orthopyroxenes; the activation energy for Mg-rich orthopyroxenes is ~251 kJ/mol, whereas that for Fe-rich ones is ~185 kJ/mol. The activation energy gap occurs between Fs50 and Fs60, which seems to correspond to the minimum in the ln K_D vs. $1/T$ curves shown in Figure 3.

The slope of the ln K_D vs. $1/T$ (K) plot between 1000 and 1200 K for the Fs25 sample is parallel to that determined by Molin et al. (1991) on quenched natural orthopyroxene from the Johnstown meteorite with $X_{Fe} = 0.233$ (Figure 2a). This similarity indicates that the ordering states below 1200 K are quenchable for Mg-rich orthopyroxenes, supporting the kinetic studies by Besancon (1981) and Anovitz et al. (1988). Hence, the relationship between ln K_D and $1/T$ determined from quenched samples below 1200 K for Mg-rich orthopyroxenes may be used reliably to obtain the so-called quenched ordering states, which are necessary for the calculation of cooling rates of host rocks and meteorites (Ganguly, 1982; Ganguly et al., 1994). However, the slopes of the ln K_D vs. $1/T$ for Fs39 and Fs51 are quite different from those calculated from the data given by Saxena and Ghose (1971) for Fs46 (sample no. 277) and Fs50 (sample no. 10) (Fig. 2b). The difference may stem from the method they used to quench the samples and measure the site occupancies; it may also result from the kinetics of the Fe-Mg order-disorder in Fe-rich orthopyroxenes being much more rapid than that in Mg-rich ones (Besancon, 1981; Anovitz et al., 1988).

TABLE 3. Comparison of ΔG_{exch}, W^{M1}, and W^{M2} (kJ/mol) values between 1000 and 1200 K

$-\Delta G_{exch}$	W^{M1} ($= \overline{W}^{M1} - \frac{1}{2}\Delta G_{rec}$)	W^{M2} ($= \overline{W}^{M2} - \frac{1}{2}\Delta G_{rec}$)	Source
15.05			Virgo and Hafner (1969)
10.49–11.06	8.01–6.86	5.08–4.42	Saxena and Ghose (1971)
10.45–11.29	7.77–5.31	5.00–3.29	Sack (1980)
8.95–14.40			Besancon (1981)
11.55–11.79	6.37	4.51	Ganguly (1982)
11.06–11.27	5.45	2.08	Anovitz et al. (1988)
13.62	4.43–3.07	6.34–4.98	Davidson and Lindsley (1989)
7.82	7.42	7.42	Sack and Ghiorso (1989)
12.50–11.90	7.70–5.70	4.20–1.70	Shi et al. (1992)
10.73–11.33	8.12–7.70	7.14–5.63	this study

Temperature dependence of ΔG_{exch}, W^{M1}, and W^{M2}

In general, the Gibbs free energy change for the exchange reaction (ΔG_{exch}) and the interaction parameters W^{M1} and W^{M2} are temperature and pressure dependent. Since all our measurements of site occupancies were conducted at 1 bar, the pressure effect on ΔG_{exch} and W are excluded from the following discussion.

The ΔG_{exch} parameter derived in this study increases, whereas both W^{M1} and W^{M2} decrease with increasing temperature (Fig. 4), suggesting that the orthopyroxene solid solution approaches ideal mixing as temperature increases. These observations are consistent with the previous experimental results (e.g., Saxena and Ghose, 1971; Anovitz et al., 1988). Table 3 is a summary of the ΔG_{exch}, W^{M1}, and W^{M2} values reported in the previous and present studies. Note that for comparison, the $\overline{W}^{M1}$ and $\overline{W}^{M2}$ values given by Sack (1980), Davidson and Lindsley (1989), Sack and Ghiorso (1989), and Shi et al. (1992) are converted into W^{M1} and W^{M2} according to Equation 6. It can be seen that the agreement for ΔG_{exch} values is excellent; however, the W^{M1} and W^{M2} values derived in this study appear to be slightly larger than those reported previously. The nonequivalence of the W^{M1} and W^{M2} values indicates that the asymmetry of the orthopyroxene solid solution exists between 1000 and 1200 K, but it is

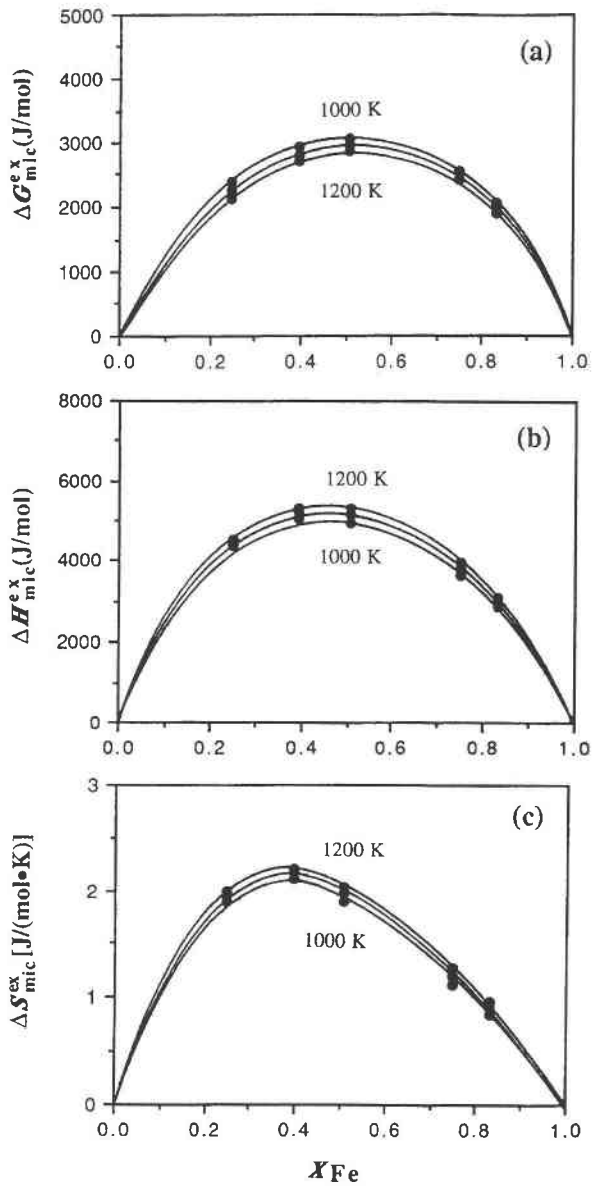

Fig. 5. Microscopic excess thermodynamic properties of the orthopyroxene solid solution as a function of composition (two-site basis): (**a**) excess Gibbs free energy vs. X_{Fe}, (**b**) excess enthalpy vs. X_{Fe}, and (**c**) excess entropy vs. X_{Fe}.

much less pronounced than that reported previously at lower temperatures.

It is interesting to note that the difference between W^{M1} and W^{M2}, namely, $W^{M1} - W^{M2}$, does not decrease with increasing temperature as found by Saxena and Ghose (1971), Sack (1980), and Ganguly (1982); instead, the difference becomes larger, in agreement with that obtained by Shi et al. (1992). This result implies that the asymmetry of the solution increases at elevated temperatures and reflects increasing dissimilarity of the atomic configurations around cations in the M1 and M2 sites, which is, in fact, what we have observed from the crystal structure studies of orthopyroxenes at high temperatures (Yang, 1994). From 296 to 1300 K for Mg-rich orthopyroxenes and from 296 to 1200 K for Fe-rich ones, the octahedral site, M1, remains nearly regular, whereas the M2 site switches one of its coordination O atoms (O3B) at high temperatures and becomes far more distorted than that at 296 K. The approach of the phase transition from orthopyroxene to its high-temperature polymorphs with increasing temperature may be responsible for the increase in the value for $W^{M1} - W^{M2}$ and the asymmetry of the solid solution in the range 1000–1200 K. Therefore, the linear extrapolation of W^{M1} and W^{M2} to lower temperatures is not warranted since the structure of orthopyroxene at lower temperatures behaves differently from that at higher temperatures.

Excess thermodynamic properties of the solution

On the basis of a sublattice solid-solution model, Shi et al. (1992) deduced the following equations for the microscopic excess thermodynamic properties of the orthopyroxene solid solution:

$$\Delta G^{ex}_{mic} = X^{M1}_{Fe} X^{M1}_{Mg} W^{M1}_{G} + X^{M2}_{Fe} X^{M2}_{Mg} W^{M2}_{G} \quad (9)$$

$$\Delta H^{ex}_{mic} = X^{M1}_{Fe} X^{M1}_{Mg} W^{M1}_{H} + X^{M2}_{Fe} X^{M2}_{Mg} W^{M2}_{H} \quad (10)$$

$$\Delta S^{ex}_{Mic} = X^{M1}_{Fe} X^{M1}_{Mg} W^{M1}_{S} + X^{M2}_{Fe} X^{M2}_{Mg} W^{M2}_{S} \quad (11)$$

and the following for the microscopic mixing properties:

$$\Delta G^{mix}_{mic} = RT(X^{M1}_{Fe} \ln X^{M1}_{Fe} + X^{M1}_{Mg} \ln X^{M1}_{Mg} + X^{M2}_{Fe} \ln X^{M2}_{Fe} + X^{M2}_{Mg} \ln X^{M2}_{Mg}) + \Delta G^{ex}_{mic} \quad (12)$$

$$\Delta S^{mix}_{mic} = -R(X^{M1}_{Fe} \ln X^{M1}_{Fe} + X^{M1}_{Mg} \ln X^{M1}_{Mg} + X^{M2}_{Fe} \ln X^{M2}_{Fe} + X^{M2}_{Mg} \ln X^{M2}_{Mg}) + \Delta S^{ex}_{mic} \quad (13)$$

$$\Delta H^{mix}_{mic} = \Delta H^{ex}_{mic}. \quad (14)$$

Figure 5 illustrates the variation of ΔG^{ex}_{mic}, ΔH^{ex}_{mic}, and ΔS^{ex}_{mic} with chemical composition at various temperatures, calculated from Equations 9–11. The ΔG^{ex}_{mic} values agree with those given by Shi et al. (1992) for Fe-rich orthopyroxenes but are slightly larger than those given for Mg-rich ones, the maximum difference being ~1.5 kJ/mol. The slightly larger ΔG^{ex}_{mic} values obtained in this work for Mg-rich orthopyroxenes may originate from the anomalous behavior of the cation ordering and structural change in Mg-rich orthopyroxenes at high temperature (Yang and Ghose, in preparation).

To calculate the macroscopic mixing properties from the site-occupancy data, we have adopted a simple mixture model (Mueller, 1962; Banno and Matsui, 1967; Thompson, 1970; Saxena and Ghose, 1971),

$$a_{Fe} = (a^{M1}_{Fe} a^{M2}_{Fe})^{1/2} \quad (15)$$

where a_{Fe} is the activity of the Fe component in $(Fe,Mg)SiO_3$ orthopyroxenes; a^{M1}_{Fe} and a^{M2}_{Fe} are the partial

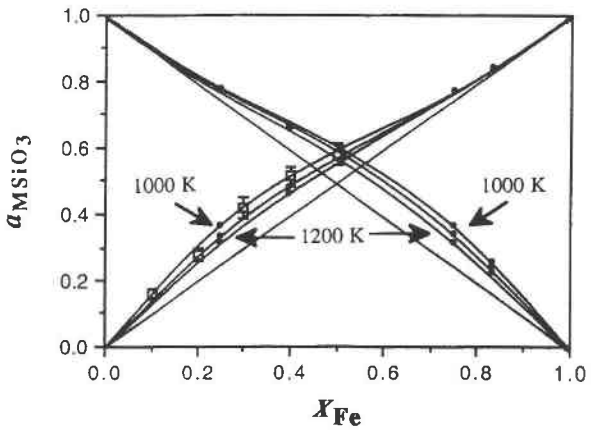

Fig. 6. The activity-composition relations for the orthopyroxene solid solution. Solid circles were calculated from our data. The activity measurements at 1477 K of Kitayama and Katsura (1968) are shown in open squares with 2σ error brackets. The ideal mixing lines are indicated for reference.

activities of Fe component on the individual M1 and M2 sites, respectively. According to Saxena and Ghose (1971),

$$a_{Fe}^{M1} = X_{Fe}^{M1}\gamma_{Fe}^{M1} \tag{16a}$$

$$a_{Fe}^{M2} = X_{Fe}^{M2}\gamma_{Fe}^{M2} \tag{16b}$$

where γ_{Fe}^{M1} and γ_{Fe}^{M2} are the partial activity coefficients for the Fe component on M1 and M2, respectively, and they are of the form

$$RT \ln \gamma_{Fe}^{M1} = W^{M1}(1 - X_{Fe}^{M1})^2 \tag{17a}$$

$$RT \ln \gamma_{Fe}^{M2} = W^{M2}(1 - X_{Fe}^{M2})^2 \tag{17b}$$

where W^{M1} and W^{M2} have the same meaning as those in Equation 3. Similar equations can be written for the Mg component.

Figure 6 shows the activity-composition relations for the solid solution calculated from Equations 15–17. The activity measurements at 1477 K by Kitayama and Katsura (1968) are also shown in Figure 6 for comparison. The nonideality of mixing is apparent, which decreases with increasing temperature. However, our results appear to show a less nonideal mixing than that presented by Kitayama and Katsura (1968).

The macroscopic excess Gibbs free energy of the $(Fe,Mg)SiO_3$ solid solution can be calculated using the equation

$$\Delta G_{mac}^{ex} = RT(X_{Fe} \ln \gamma_{Fe} + X_{Mg} \ln \gamma_{Mg}) \tag{18}$$

where

$$\gamma_{Fe} = \frac{[(X_{Fe}^{M1}\gamma_{Fe}^{M1})(X_{Fe}^{M2}\gamma_{Fe}^{M2})]^{1/2}}{X_{Fe}} \tag{19a}$$

$$\gamma_{Mg} = \frac{[(X_{Mg}^{M1}\gamma_{Mg}^{M1})(X_{Mg}^{M2}\gamma_{Mg}^{M2})]^{1/2}}{X_{Mg}} \tag{19b}$$

and the macroscopic Gibbs free energy of mixing can be calculated from the equation

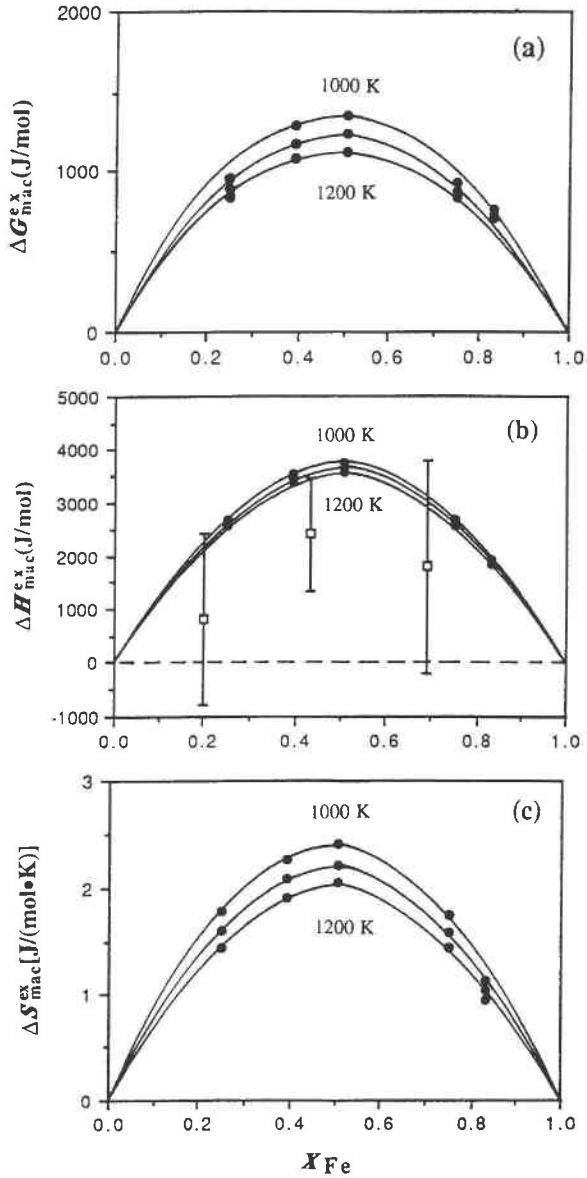

Fig. 7. Macroscopic excess thermodynamic properties of the orthopyroxene solid solution as a function of composition (one-site basis): (**a**) excess Gibbs free energy vs. X_{Fe}, (**b**) excess enthalpy vs. X_{Fe}. The data indicated by open squares with 2σ error bars represent the solution calorimetric values at 1023 K of Chatillon-Colinet et al. (1983). (**c**) Excess entropy vs. X_{Fe}.

$$\Delta G_{mac}^{mix} = RT(X_{Fe} \ln a_{Fe} + X_{Mg} \ln a_{Mg}). \tag{20}$$

The ΔS_{mac}^{ex}, ΔS_{mac}^{mix}, and $\Delta H_{mac}^{ex} = \Delta H_{mac}^{mix}$ can be obtained from the general thermodynamic formulae

$$\Delta S = -(\partial \Delta G/\partial T)_P \tag{21}$$

$$\Delta H = [\partial(\Delta G/T)/\partial(1/T)]_P. \tag{22}$$

The calculated ΔG_{mac}^{ex}, ΔS_{mac}^{ex}, ΔH_{mac}^{ex}, and ΔG_{mac}^{mix} values of the solid solution as a function of composition are shown in Figures 7 and 8, respectively. The data from the ca-

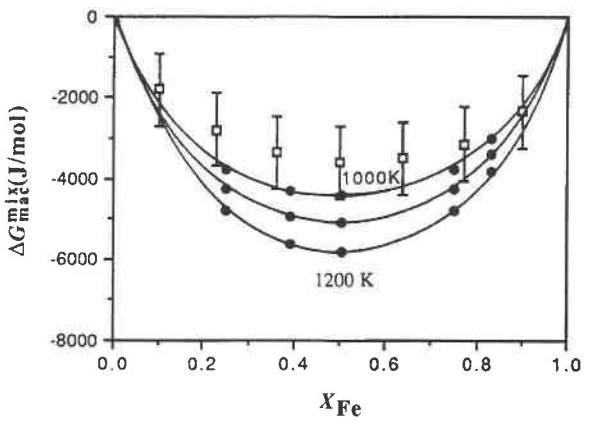

Fig. 8. Macroscopic Gibbs free energy of mixing vs. composition (one-site basis). Open squares with 2σ error brackets are from the EMF measurements at 1000 K of Sharma et al. (1987).

lorimetric measurements of the excess enthalpy at 1023 K by Chatillon-Colinet et al. (1983) and the EMF measurements of the Gibbs free energy of mixing at 1000 K by Sharma et al. (1987) are also plotted in Figures 7b and 8, respectively. The agreements between our data and those determined experimentally for ΔH^{ex}_{mac} (Chatillon-Colinet et al., 1983) and ΔG^{mix}_{mac} (Sharma et al., 1987) are reasonably good, indicating that the thermodynamic mixing properties of orthopyroxenes can be adequately described by a regular solution type formulation.

From the calorimetric measurements of the solid solution, Chatillon-Colinet et al. (1983) calculated the disordering enthalpy, which is 7100 J/mol between natural and experimentally disordered orthopyroxene ($En_{52.5}Fs_{47.5}$). Unfortunately, the ordering states of the samples they studied are unknown. Ganguly (1986) derived an equation for the calculation of the disordering enthalpy in minerals. For orthopyroxenes, the equation is of the form

$$\Delta H^{dis} = [X^{M1}_{Mg}(\zeta_0) - X^{M1}_{Mg}(\zeta)] \times \{\Delta H_{exch} - (1 - 2X_{Mg})(W^{M2} - W^{M1}) + (W^{M1} + W^{M2})[X^{M1}_{Mg}(\zeta_0) + X^{M1}_{Mg}(\zeta) - 2X_{Mg}]\} \quad (23)$$

where $X^{M1}_{Mg}(\zeta_0)$ and $X^{M1}_{Mg}(\zeta)$ are the site occupancies of the natural and heat-treated samples, respectively; X_{Mg} is the total mole fraction of Mg in the samples, and ΔH_{exch} is the enthalpy for the exchange reaction (Eq. 2b). Using Equation 23 and our data on Fs_{51} and assuming a linear relationship between ln K_D and $1/T$ within the temperature range 600–1300 K, we obtained a value of ~3500 J/mol for the disordering enthalpy of mixing. This value is about half that given by Chatillon-Colinet et al. (1983) but very similar to the value of 3347 J/mol estimated by Anovitz et al. (1988). However, on the basis of our data, it seems that Chatillon-Colinet et al. (1983) slightly overestimated the ordering state of the sample they experimentally disordered. If we assume a linear relationship between ln K_D and $1/T$ (K), the estimated ordering states for the sample studied by Chatillon-Colinet et al. (1983) are $X^{M1}_{Mg}(\zeta_0) = 0.864$ and $X^{M1}_{Mg}(\zeta) = 0.703$ at 600 and 1300 K, respectively. By taking their values of $\Delta H_{exch} = 31.35$ kJ/mol and $W_H = 7.94$ kJ/mol, we estimate the disordering enthalpy of mixing of their sample to be ~6.30 kJ/mol using Equation 23.

Acknowledgments

This research would not have been possible without the generosity of D.H. Lindsley, SUNY, Stony Brook, in whose laboratory most of the orthopyroxene samples were synthesized with his participation. We have benefited from discussions with M.S. Ghiorso, J. Ganguly, and R.O. Sack. We are grateful to W.D. Scott for his help in modifying the high-temperature furnace, to M.J. Brown and M. Cai for providing the facilities for the evacuation and sealing of crystal mounts, to H. Ohashi of Tsukuba, Japan, for providing the Fs40 sample, and to L.W. Finger for providing the RFINE90 program. The support of this research by the grants from NASA (NAG9-460 to J. Ganguly and S.G.), NSF (EAR-9117389 to S.G.), and the University of Washington Department of Geological Sciences Graduate Research Fund is gratefully acknowledged.

References cited

Akamatsu, T. (1989) Intracrystalline cation distribution in the major mantle minerals and its significance for the state of materials in the Earth. Journal of the Earth Sciences, Nagoya University, 36, 185–322.

Anovitz, L.M., Essene, E.J., and Dunham, W.R. (1988) Order-disorder experiments on orthopyroxenes: Implications for the orthopyroxene geospeedometer. American Mineralogist, 73, 1060–1073.

Banno, S., and Matsui, Y. (1967) Thermodynamic properties of intracrystalline exchange solid solution. Proceedings of the Japan Academy, 43, 762–767.

Besancon, J. R. (1981) Rate of cation ordering in orthopyroxenes. American Mineralogist, 66, 965–973.

Chatillon-Colinet, C., Newton, R.C., Perkins, D., III, and Kleppa, O.J. (1983) Thermochemistry of (Fe^{2+},Mg) orthopyroxene. Geochimica et Cosmochimica Acta, 47, 1597–1603.

Davidson, P.M., and Lindsley, D.H. (1985) Thermodynamic analysis of quadrilateral pyroxenes. II. Model calibration from experiments and application to geothermometry. Contributions to Mineralogy and Petrology, 91, 390–404.

——— (1989) Thermodynamic analysis of pyroxene-olivine-quartz equilibrium in the system CaO-MgO-FeO-SiO_2. American Mineralogist, 74, 18–30.

Domeneghetti, M.C., Molin, G.M., and Tazzoli, V. (1985) Crystal-chemical implications of the Mg^{2+}-Fe^{2+} distribution in orthopyroxenes. American Mineralogist, 70, 987–995.

Enck, D.E., and Dommel, G. (1965) Behavior of the thermal expansion of NaCl at elevated temperatures. Journal of Applied Physics, 36, 839–844.

Evans, B.J., Ghose, S., and Hafner, S. (1967) Hyperfine splitting of Fe^{57} and Mg-Fe order-disorder in orthopyroxenes ($MgSiO_3$ solid solution). Journal of Geology, 75, 306–322.

Finger, L.W., and Prince, E. (1975) A system of Fortran IV computer program for crystal structure computations. NBS Technical Note 854, National Beureau of Standards, Washington, DC.

Ganguly, J. (1982) Mg-Fe order-disorder in ferromagnesian silicates. II. Thermodynamics, kinetics and geological applications. In S.K. Saxena, Ed., Advances in physical geochemistry, vol. 2, p. 58–99. Springer-Verlag, New York.

——— (1986) Disordering energy versus disorder in minerals: A phenomenological relation and application to orthopyroxene. Journal of Physics and Chemistry of Solids, 47, 417–420.

Ganguly, J., Yang, H., and Ghose, S. (1994) Thermal history of mesosiderites: Constraints from compositional zoning and Fe-Mg ordering in orthopyroxenes. Geochimica et Cosmochimica Acta, in press.

Ghose, S. (1965) Mg^{2+}-Fe^{2+} order in an orthopyroxene, $Mg_{0.93}Fe_{1.07}Si_2O_6$. Zeitschrift für Kristallographie, 122, 81–99.

Ghose, S., and Hafner, S. (1967) Mg^{2+}-Fe^{2+} distribution in metamorphic and volcanic orthopyroxenes. Zeitschrift für Kristallographie, 125, 1–6.

Hawthorne, F.C., and Ito, J. (1977) Synthesis and crystal-structure refinement of transition-metal orthopyroxenes. I. Orthoenstatite and (Mg,Mn,Co) orthopyroxenes. Canadian Mineralogist, 15, 321–338.

Hazen, R.M., and Finger, L.W. (1982) Comparative crystal chemistry, p. 231. Wiley, New York.

Hazen, R.M., Finger, L.W., and Ko, J. (1993) Effects of pressure on Mg-Fe ordering in orthopyroxene synthesized at 11.3 GPa and 1600 °C. American Mineralogist, 78, 1336–1339.

Ibers, J.A., and Hamilton, W.C., Eds. (1974) International tables for X-ray crystallography, vol. 4, 366 p. Kynoch, Birmingham, U.K.

Kitayama, K., and Katsura, T. (1968) Activity measurements in orthosilicate and metasilicate solid solutions. I. Mg_2SiO_4-Fe_2SiO_4 and $MgSiO_3$-$FeSiO_3$ at 1204 °C. Bulletin of the Chemical Society of Japan, 41, 1146–1151.

Molin, G.M. (1989) Crystal-chemical study of cation distribution in Al-rich and Al-poor orthopyroxenes from spinel lherzolite xenoliths. American Mineralogist, 74, 593–598.

Molin, G.M., Saxena, S.K., and Brize, E. (1991) Iron-magnesium order-disorder in an orthopyroxene crystal from Johnstown meteorite. Earth and Planetary Science Letters, 105, 260–265.

Mueller, R.F. (1962) Energetics of certain silicate solid solution. Geochimica et Cosmochimica Acta, 26, 581–598.

Navrotsky, A. (1971) The intracrystalline cation distribution and the thermodynamics of solid solution formation in the system $FeSiO_3$-$MgSiO_3$. American Mineralogist, 56, 201–211.

Sack, R.O. (1980) Some constraints on the thermodynamic mixing properties of Fe-Mg orthopyroxenes and olivines. Contributions to Mineralogy and Petrology, 71, 257–269.

Sack, R.O., and Ghiorso, M.S. (1989) Importance of considerations of mixing properties in establishing an internally consistent thermodynamic database: Thermochemistry of minerals in the system Mg_2SiO_4-Fe_2SiO_4-SiO_2. Contributions to Mineralogy and Petrology, 102, 41–68.

Saxena, S.K., and Ghose, S. (1970) Order-disorder and the activity-composition relation in a binary crystalline solution. I. Metamorphic orthopyroxene. American Mineralogist, 55, 1219–1225.

——— (1971) Mg^{2+}-Fe^{2+} order-disorder and the thermodynamics of the orthopyroxene crystalline solution. American Mineralogist, 56, 532–559.

Saxena, S.K., Domeneghetti, M.C., Molin, G.M., and Tazzoli, V. (1989) X-ray diffraction study of Fe^{2+}-Mg order-disorder in orthopyroxene. Some kinetic results. Physics and Chemistry of Minerals, 16, 421–427.

Sharma, K.C., Agrawal, R.D., and Kapoor, M.L. (1987) Determination of thermodynamic properties of (Fe,Mg)-pyroxenes at 1000 K by the emf method. Earth and Planetary Science Letters, 85, 302–310.

Shi, P., Saxena, S.K., and Sundman, B. (1992) Sublattice solid solution model and its application to orthopyroxene $(Mg,Fe)_2Si_2O_6$. Physics and Chemistry of Minerals, 18, 393–405.

Skogby, H. (1992) Order-disorder kinetics in orthopyroxenes of ophiolite origin. Contributions to Mineralogy and Petrology, 109, 471–478.

Smyth, J.R. (1974) The high-temperature crystal-chemistry of clinohypersthene. American Mineralogist, 59, 1069–1082.

Snellenburg, J.W. (1975) Computer simulation of the distribution of octahedral cations in orthopyroxene. American Mineralogist, 60, 441–447.

Sykes, J., and Molin, G.M. (1986) Structural variations in orthopyroxenes. International Mineralogical Association Abstracts with Program, 14, 243.

Sykes-Nord, J.A., and Molin, G.M. (1993) Mg-Fe order-disorder in Fe-rich orthopyroxenes: Structural variations and kinetics. American Mineralogist, 78, 921–931.

Thompson, J.B., Jr. (1970) Chemical reactions in crystals. Corrections and clarifications. American Mineralogist, 55, 528–538.

Tsukimura, K., Sato-Sorensen, Y., Ghose, S. (1989) A gas-flow furnace for x-ray crystallography. Journal of Applied Crystallography, 22, 401–405.

Turnock, A.C., Lindsley, D.H., and Grover, J.E. (1973) Synthesis and unit cell parameters of Ca-Mg-Fe pyroxenes. American Mineralogist, 58, 50–59.

Virgo, D., and Hafner, S.S. (1969) Order-disorder in heated orthopyroxenes. Mineralogical Society of America Special Paper, 2, 67–81.

Yang, H. (1994) High temperature single-crystal x-ray diffraction studies of synthetic iron-magnesium orthopyroxenes: Thermal expansion, crystal structure and thermodynamic properties. Ph.D. thesis, University of Washington, Seattle, Washington.

Yang, H., and Ghose, S. (1994) Thermal expansion, Debye temperature and Grüneisen parameter of synthetic $(Fe,Mg)SiO_3$ orthopyroxenes. Physics and Chemistry of Minerals, in press.

Zachariasen, W.Y. (1968) Extinction and Boorman effects in mosaic crystals. Acta Crystallographica, A28, 421–424.

Manuscript received November 18, 1993
Manuscript accepted March 25, 1994